EXPERIMENTS ON INTENSE ELECTRON BEAM TRANSPORT IN MESH FOCUSING ARRAYS

-Stanley Humphries, Jr.+
Acceleration Consultants
Albuquerque, New Mexico 87122

and

Carl Ekdahl
Los Alamos National Laboratory
Los Alamos, New Mexico 87545

ABSTRACT

We describe recent experiments on the transport of high-current relativistic electron beams in vacuum using wire-mesh focusing. We observed self-contained propagation of 44 kA beams at a maximum energy of 3 MeV - the corresponding value of ν/γ was ~0.4. The experiments are a one-hundred-fold extrapolation of beam power over our previous results. The beam behavior was in close agreement with theory. The results show that mesh focusing has application to the most intense electron beams presently available from pulsed power generators.

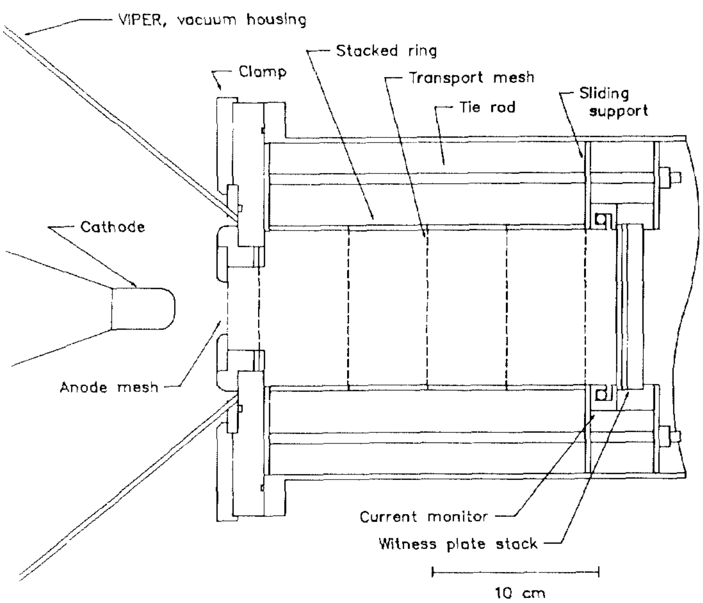

Fig. 1. Scale drawing of the transport hardware on the VIPER generator.

EXPERIMENTAL APPARATUS

We carried out experiments in two runs on the VIPER generator at Los Alamos National Laboratory and SUPER-IBEX at the Naval Research Laboratory. Fig. 1 shows the transport hardware. The beam entered a cylindrical tube interrupted by a series of transverse meshes. The meshes reduced the radial electric field of the relativistic electron beam allowing the magnetic pinching force to dominate [1-4]. The beam propagated in a self-contained equilibrium. The vacuum chamber, consisting of 20 cm stainless steel pipes, supported the mesh transport system. The 9.6 cm diameter transport assembly consisted of spacer rings and special notched rings. We fabricated high transparency meshes on the notched rings with 0.013 cm diameter wire. Hardware limited the number of cells to sixteen.

We used toroidal magnetic pickup coils to measure the net beam current. The beams carried enough energy to produce significant damage in witness plates. The wire meshes survived shots with beam current in the range 10-20 kA. More intense beams melted holes through the centers of the meshes. We could estimated the beam radius and centroid location from wire damage. X-ray pinhole photographs provided an independent measurement of the beam profile at the end of the system.

The current pulse from VIPER had a full-width at half-maximum (FWHM) of 76 ns. On most shots, the net diode current was 30 kA with a 1.4 MV peak voltage. The recently installed SUPER-IBEX generator had diode parameters of 80 kA and 3 MV with a 43 ns current pulse.

EXPERIMENTAL RESULTS, VIPER

To begin experiments, we took several shots to visualize the beam entering the transport system and to demonstrate capture of a self-pinched beam. An acrylic target 4 cm behind the anode mesh showed a 2 cm diameter melt region. The witness plate verified that the VIPER diode produced a well-defined self-pinched beam. We measured the net input current at a point 3 cm from the anode foil. The entering current showed good reproducibility with little dependence on the geometry of the downstream transport system. The input current to the transport system was about 27 kA, close to the full machine current. The total energy of the beam was about 2 kJ.

Most of the shots in the VIPER run were devoted to high current propagation in short cells. We used brass witness plates on a range-thick stainless steel conversion plate for X-ray pinhole photographs of the beam. For all system geometries, we took shots with and without the transport meshes to gauge the success of mesh transport. Fig. 2 shows measurements of net current in a transport system with six 4 cm cells. In Shot 017, the current monitor was in the first cell, while the monitor in Shot 011 measured the current in the final cell. At peak voltage, about 27 kA reached the end plate of the mesh focusing

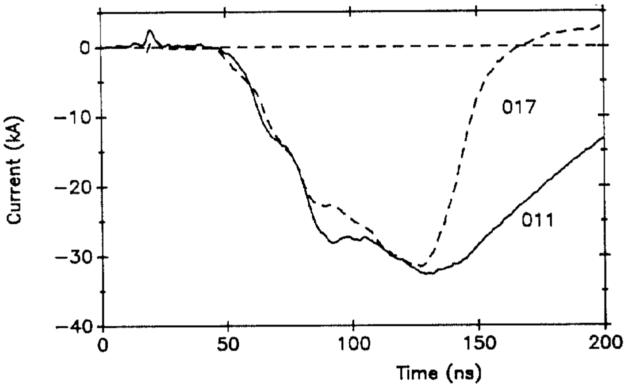

Fig. 2. Entrance (017) and exit (011) current, six cells, 4 cm length.

array, about 90 per cent of the available machine current. Within the accuracy of the measurement, the system captured all current that entered the first cell. The beam melted a 2.8 cm diameter region of a brass witness plate at the end of the transport system. Calculations of the energy for melting shows that the net current in the region exceeded 19 kA. Some of the current was contained in a beam halo - the brass plate was thermally discolored over a 5 cm diameter region. The halo diameter was about half the diameter of the transport tube.

We took a shot (012) for the same diode and tube geometry with all meshes removed. There was a substantial difference in the nature of transported current. With no meshes, the strong space charge potential caused rapid expansion of the beam. Fig. 3 shows net current measurements at the end of the 24 cm system. Without meshes, the current in the final cell dropped to 13 kA - half the current struck the wall of the transport tube. Also, the current reached a maximum value at the peak of the voltage and dropped as longitudinal space-charge effects increased in importance. The witness plates also showed a strong difference - the plate for Shot 012 had no thermal damage.

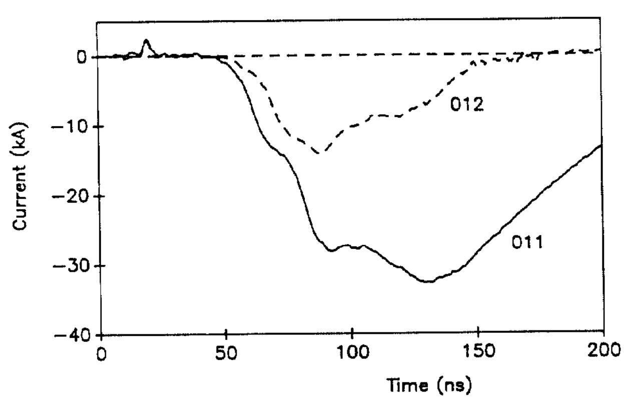

Fig. 3. Net current at end of transport system. a) Shot 011, 6 cells, 4 cm length. b) Shot 012, 1 cell, 24 cm length.

Photographs taken with a time-integrated X-ray pinhole camera provided another basis of comparison. On Shot 011 with meshes, the X-ray distribution showed that electron loss on the wall of the transport tube was very small. We saw a bright image of a strongly-pinched beam at the end plate. With no meshes, the photograph showed enhanced electron loss near the diode and wall losses along the length of the transport tube. A diffuse beam filled image the full diameter of the end plate.

We also took shots to achieve high values of transported current. For these shots, the VIPER diode voltage was about 1.9 MV and the available current increased to 44 kA. The transport system consisted of 13 cells of length 3 cm. In these shots, we experienced problems with current monitor shorting - we had to rely on witness plates for qualitative measurements. From the increased damage, it was apparent that the transported current was substantially higher than previous shots. The beam melted a clean hole through all 12 wire assemblies as well the brass witness plate. The beam traveled in a straight line - the holes in the wires and plate were well-aligned along the axis of the transport tube. From the melt region in the brass plate, we estimated a minimum current in the beam core of 34 kA. With no meshes, the brass plate was thermally discolored over its full diameter but not melted.

Because of limited hardware, we could not extend the 3 cm cells to a distance longer than 48 cm. We had to use longer cells for a longer transport system. Predictions with the FTRAN code [5] showed that we could not carry the full available current from VIPER with longer cells because of the high space-charge potential. With 9 cm cells, we observed strong beam loss in the first cell and transport of about 7 kA. For these parameters, the X-ray pinhole photographs gave a clear view of a self-pinched beam equilibrium. The current that remained had low emittance and propagated with negligible wall loss. We observed a well-centered, narrow pinched beam at the end plate with a Gaussian profile with a radius (at half-maximum) of only 1 cm.

EXPERIMENTAL RESULTS, SUPER-IBEX

The SUPER-IBEX generator provided a high current electron beam with fast risetime. In most shots, we used short cells (3 cm) to transport a high fraction of the machine current. The transport system had sixteen cells. Fig. 4 shows net current measurements at the entrance and exit of the transport system for a shot with a 13 μm titanium anode foil (Shot 180). The system captured and transported about half the available machine current. The entrance monitor showed a peak current of 57 kA, about 73 per cent of the machine current. The peak current at the exit was 44 kA. There were two reasons for reduced capture and transport efficiency on SUPER-IBEX compared with VIPER. First, diode simulations predicted a halo of high divergence electrons in the entering beam. Second, the anode foil and coarse meshes that we used to mate the transport system to the machine increased the emittance of the incident beam.

A brass witness plate at the end of the system showed a melt region 3 cm in diameter. Thermal damage extended over a 5 cm circle. The melting criterion predicted a current exceeding 37 kA. The beam punched holes through the first nine meshes - the diameter of the holes was 2 to 3 cm near the entrance and decreased in size moving downstream. The last six meshes were not melted. The pattern of damage suggests that the beam expanded as it propagated. We attribute expansion to the high entrance emittance of the beam.

Fig. 5 shows comparative data for a shot with the same geometry but with no meshes. The figure illustrates net current at the entrance and exit. Only 14 kA of the 54 kA that entered reached the end of the system. The pulselength of the exit current (FWHM) was 19 ns - only high energy electrons reached the end. We found no visible damage to a brass witness plate at the end of the 48 cm system.

We found that the input beam emittance had a strong influence on the formation of a self-pinched beam. In Shot 174, we used a 38 μm titanium anode foil rather than the 13 μm foil of Shot 180. The transport geometry and injected beam were otherwise identical. With a thick anode foil, the magnitude of the transported current and the pulse-width were smaller. We observed a dramatic difference in witness plate damage. The high emittance beam of Shot 174 had a larger radius and left the mesh wires intact. There was no visible damage to the brass witness plate - a thin sheet of radiochromic film on the witness plate was not melted. The exposure of the film showed a diffuse beam spread over the diameter of the

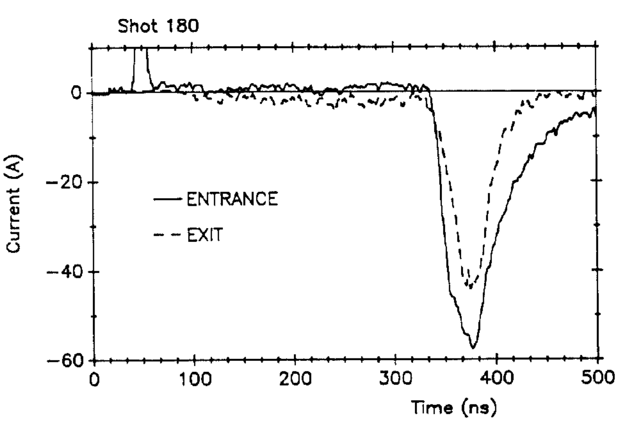

Fig. 4. Net beam current at entrance to and exit from transport system. 16 cells, 3 cm length. 13 μm Ti anode foil.

It is significant to note that the beam propagated close to the longitudinal space charge limit in the high current shots. The space-charge potential in all sixteen cells approached 2 MV, while the electric field on the mesh wires exceeded 100 MV/m. Despite the high fields, we observed no evidence of breakdown. The field polarity on the wires repelled surface electrons - initiation of a breakdown would require direct extraction of ions from the surface.

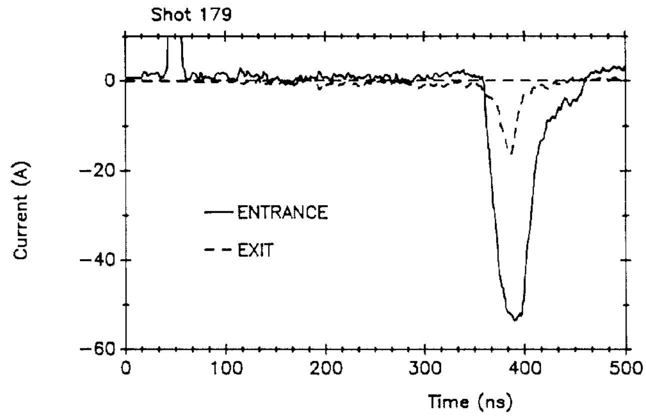

Fig. 5. Net beam current at entrance to and exit from transport system. 1 cell, 48 cm length. 13 μm Ti anode foil.

We also performed experiments with a long system consisting of sixteen cells with average length 8 cm. The highest transported current was about 10 kA, consistent with the predictions from FTRAN. Because of the high angular divergence of the injected beam, we did not achieve the tight pinches observed in the VIPER experiments.

We conclude that transverse wire meshes can transport high ν/γ relativistic electron beams. With proper diode design and the replacement of anode foils with high-transparency meshes, we feel that we can achieve close to 100 per cent capture and transport of available current from high power generators. We are currently carrying out studies with EBQ [6] to design systems for optimum matching.

ACKNOWLEDGMENTS

We would like to thank H.A. Davis and other members of Group P-1 at Los Alamos National Laboratory for contributions of time for the experiments and invaluable help in running the VIPER machine. We would also like to thank R. Meger and J. Antoniades of the Naval Research Laboratory for the contribution of time for experiments, effort in preparing their new machine, and help with data acquisition. This work was supported by the Department of Energy, Defense Advanced Research Projects Agency, and the Office of Naval Research.

REFERENCES

+ Permanent address, University of New Mexico, Albuquerque, New Mexico 87131.

1. R.J. Adler, Part. Accel. 12, 263 (1980).
2. R.J. Adler, B. Sabol and G.F. Kiuttu, IEEE Trans. Nucl. Sci. NS-30, 3198 (1983).
3. S. Humphries, Jr., Part. Accel. 13, 249 (1983).
4. S. Humphries, Jr. and C. Ekdahl, J. Appl. Phys. 63, 583 (1988).
5. S. Humphries, Jr., "Design of Foil Transport Systems," (Acceleration Consultants, ACCON-88-03, 1988).
6. A.C. Paul, "EBQ Code" (Lawrence Berkeley Labortory, LBL-13241, 1982).